Analysis Note for 60H Dataset Relative Unblinding

Nick Kinnaird - Boston University

January 23, 2019

High Level Summary

- Lead Analysts: Nick Kinnaird, James Mott
- Positron Reconstruction Method: Recon West
- Software Release: V9_11_00
- Dataset: gm2pro_daq_full_run1_60h_5033A_withfullDQC
- Histogramming Method: Ratio
- Gain Correction Method: Default in reconstruction
- Pileup Correction Method: Asymmetic shadow window, doublets only
- Lost Muon Spectrum Extraction: Triple coincidence, not included in ratio fit
- Model for CBO: Exponential envelope, frequency from tracking analysis
- Model for VW: Exponential envelope, constant frequency, not included in ratio fit
- Fit Range: $30\,\mu\text{s} - 500\,\mu\text{s}$
- $R = -19.88 \pm 1.373\,\text{ppm} \pm syst.$ (blinding with common string)
- $\chi^2/NDF = 3052/3145$
- P value = 0.8806

Final fit function:

$$R(t) = \frac{2f(t) - f_+(t) - f_-(t)}{2f(t) + f_+(t) + f_-(t)}$$

$$f_\pm(t) = f(t \pm T_a/2)$$

$$f(t) = C(t)(1 + A\cos(\omega_a t + \phi))$$

$$C(t) = 1 + A_{cbo} e^{-t/\tau_{cbo}} \cos(\omega_{cbo}(t)t + \phi_{cbo})$$

$$\omega_a = 2\pi \cdot 0.2291\,\text{MHz} \cdot (1 + R \times 10^{-6})$$

Chapter 1

Introduction

This report details the analysis procedures, results, and systematic studies I carried out for the "60H" dataset acquired during Run 1 in 2018 of the Fermilab Muon $g-2$ Experiment, E989. The 60H dataset was gathered from April 22nd, 2018 to April 24th, 2018, with runs 15921 - 15992. The quad voltages used were 13.1 and 18.3 kV, corresponding to an effective n value of 0.10843 (Cite DocDB 11547? Or find a newer reference?). The kicker voltage range was 128 - 132 kV. Nearly 1×10^9 positrons were collected during this period, corresponding to about 10% of the BNL statistics gathered. (Cite DocDB 14071 by James?)

In Chapter 2 I detail the analysis procedures used. This includes information on how the data is prepared, starting after the "production" stage and leading up to the construction of histograms. The application of gain corrections, pileup construction, the extraction of lost muons, and other various data preparation procedures are described briefly. Also included are various models used in the fitting of the data, including coherent betatron (CBO) effects and the lost muon function.

In Chapter 3 I detail the results of the analysis. This includes the application of the pileup correction, the fits to the data and subsequent residuals and FFTs of those residuals, and start time scans. Results are shown both for all calorimeters added together and for individual calorimeters.

In Chapter 4 I detail the results of systematic studies to the data and fits, which is the real meat of the analysis. This includes studies relating to corrections applied (gain, pileup, etc.), as well as models used within the fit (CBO, lost muons, VW, etc.). Also included are various studies related to items like the bin width or randomization used in the analysis.

Chapter 5 simply concludes the final results of the report, as well as next steps for the analysis. There is also an Appendix A which provides some derivations for the ratio method used in fitting the data.

Chapter 2

Analysis Procedures

2.1 Key parameters in reconstruction method

Default parameters used in the Recon West production of the 60H dataset, with SAM dataset name "gm2pro_daq_full_run1_60h_5033A_withfullDQC".

2.2 Analysis Data Preparation Procedure

- git branch: gm2analyses branch feature/KinnairdAnalyses
- Majority of code located under gm2analyses/macros/RatioMacro

1. Submit jobs to OSG to run the rootTreesAndLostMuons.fcl file which produces root trees of positron hits using the ClusterTree analyzer module and coincident MIP hits using the TestCoincidenceFinder analyzer module.
2. Submit jobs to Fermigrid to produce histograms from root trees using the ClusterTreeToHistsPileup.C macro in RatioMacro/HistMaking. Beyond standard threshold histograms this macro produces pileup and lost muon histograms all within the same root file.

2.3 Histogramming Procedure

Method: Weighted Ratio (threshold)

1. Loop through all clusters and apply an artificial deadtime (ADT) to combine hits within 6 ns into a single pulse using the same procedure and code that the pileup method uses (see below). Drop clusters with time $< 25\,\mu$s or time $> 600\,\mu$s.
2. Histograms are constructed with ROOT's TH1F class with 149.15 ns bins from $0 - 699.960\,95\,\mu$s corresponding to 4693 bins.
3. Randomize times by $\pm 149.15/2$ ns and fill histograms for energies > 1.7 GeV. Randomization uses ROOT's default TRandom3 class.
4. Fill one of the four histograms $\{u_+(t), u_-(t), v_1(t), v_2(t)\}$ as shown in Equation A.18 per cluster. The associated histogram is determined by generating a random number between 0 and 1, and comparing that number to the relative probabilities of the different weights.

5. Clusters filled into the $u_+(t)$ histogram have their times shifted by $t \to t - T_a/2$ and clusters filled into the $u_-(t)$ histogram have their times shifted by $t \to t + T_a/2$.

6. T_a is known a priori to high precision from the previous experiment, and its value is taken as $1/f_a$, where f_a is 0.2291 MHz:

$$T_a \approx 4.364\,906\,\mu\text{s} \tag{2.1}$$

2.4 Gain Correction Procedure

Gain correction method: Default by the Italian Calibration Team

1. Long term gain is corrected using out-of-fill lasers included normalization from the Source Monitor.

2. In-fill gain is corrected using in-fill lasers including normalization from the Source Monitor.

3. Short-term double pulse (SDTP) effect is not included.

2.5 Pileup Correction Procedure

Pileup correction method: Asymmetric shadow window

1. Create a vector of clusters per calorimeter per fill. For each cluster look for a second cluster in a window from 12-18 ns after the time of the first cluster. This corresponds to a shadow dead time (SDT) of 6 ns and a shadow gap time (SGT) of 12 ns, equal to 1 and 2 times the applied ADT respectively.

2. Create shadow doublets with energies and times as:

$$E_{doublet} = C \cdot (E_1 + E_2), \tag{2.2}$$

$$t_{doublet} = \frac{t_1 * E_1 + (t_2 - SGT) * E_2}{E_1 + E_2}, \tag{2.3}$$

where the latter equation is just the energy-weighted time between the two singlets. In the former equation, the calculation of the doublet energy is the sum of the singlets times some factor. That factor is set equal to 1, which is a decent approximation since the spatial separation in the reconstruction is turned off, and because the Short Term Double Pulse (SDTP) improvement to the laser energy calibration will be applied. The systematic effects of a factor not equal to 1 are studied in Section 4.2.2.

3. Randomize $t_{doublet}$ times by $\pm 149.15/2$ ns as in the histogramming procedure described above.

4. For each calorimeter construct a pileup spectrum P = doublets - singlets = D - S, where the singlets are subtracted at time $t_{doublet}$ as opposed to their individual times, and pulses are only added or subtracted if they are above 1.7 GeV. Subtract P off energy and threshold histograms.

5. For pileup subraction in the ratio method, randomly split associated doublets and singlets into 4 separate histograms as is done in the histogramming procedure described above, with times shifted accordingly. Subtract 4 pileup histograms off corresponding $\{u_+(t), u_-(t), v_1(t), v_2(t)\}$ histograms before forming the ratio.

6. The errors of the pileup corrected histogram were determined to be:

$$\sigma(N_{corrected}) = \sqrt{N_{corrected} + 2N_1 + 6N_4}, \tag{2.4}$$

   where N_1 is the number of doublets where both singlets were below threshold, and N_4 is the number of doublets where both singlets were above threshold, and this is a quantity evaluated at each time bin. (Cite this? DocDB 14830. Derive this in the appendix?) A histogram of error multipliers was created by factoring out the $N_{corrected}$ term, which is then applied to the bin errors before fitting. This is true even for the ratio errors to good approximation. (Cite this? Derive it as JP did?) Note that I did not time randomize the N_1 and N_4 entries when constructing the correct errors, which should have a negligble effect.

7. The pileup correction at the triplet/contamination level is not included. The machinery exists to apply such a correction, but it requires more work to get it correct. It has been determined not be necessary for the 60H and Run 1 data.

2.6 Lost muon spectrum extraction procedure

Method: Triple coincidence of clusters

Note that the lost muons are not included in the ratio fit because the ratio method divides out such slow effects. This is reflected by the lack of a low frequency peak in the FFT of the fit residuals for the ratio fit, whereas such a peak exists for T method fits. I include here however my method for extracting the lost muon function for possible future systematic studies.

1. Triple coincidence of clusters in 3 consecutive calorimeters are made with an energy cut of 100 MeV $<$ E $<$ 250 MeV and 5 ns $<$ dt $<$ 8.5 ns.

2. A time histogram is made with the muon cluster in the first calorimeter.

3. The function that would be used in the final fit is:

$$\Lambda(t) = 1 - \kappa_{loss} \int_0^t L(t') e^{(-t'/\gamma\tau_\mu)} dt' \tag{2.5}$$

where $L(t)$ is the triples histogram, and an arbitrary 10^{-6} factor has been absorbed into κ_{loss} in order to bring it to a more reasonable value (from $\mathcal{O}(10^{-10})$ to $\mathcal{O}(10^{-4})$).

2.7 Beam Dynamics: CBO Model

1. The CBO frequency as a function of time is taken from the tracking analysis, DocDB 14208. The CBO frequency is not constant because the quad voltage was not constant as a function of time. As described in that DocDB, the source of this is almost certainly the fact that some of the quad resistors were damaged, leading to longer RC time constants. The form used is

$$\omega_{cbo}(t) = \omega_0(1 + \Delta\omega t + Ae^{-t/\tau_A} + Be^{-t/\tau_B}) \tag{2.6}$$

with parameters determined from station 12 in the 60H dataset and fixed in the fit as:

$$\begin{aligned} \Delta\omega &= 1.86 \times 10^{-8}\,\mathrm{ns}^{-1}, \\ A &= -0.0504, \\ \tau_A &= 73.3\,\mu\mathrm{s}, \\ B &= -0.131, \\ \tau_B &= 16.6\,\mu\mathrm{s}. \end{aligned}$$

The parameter ω_0 is allowed to float in the fit and starts with a value of $2.3051\,\mathrm{rad}\,\mu\mathrm{s}^{-1}$. The ratio method has trouble with letting the other parameters float, and fixing them to various values does not change the fit results significantly.

2. Because the ratio method divides out the CBO partially (reduction by a factor of ~ 5 in the FFT cbo peak amplitude), the ratio fit has a hard time fitting the CBO lifetime. Therefore τ_{cbo} is fixed to $180\,\mu$s, determined from a T Method fit to the same data.

3. An exponential function is assumed for the CBO decoherence.

4. The N_{cbo} term is included in the fit, A_{cbo} and ϕ_{cbo} are excluded. The 2CBO term is excluded.

5. The final CBO function is:

$$N_{cbo}(t) = C(t) = 1 + A_{cbo} e^{-t/\tau_{cbo}} \cos(\omega_{cbo}(t) t + \phi_{cbo}) \tag{2.7}$$

2.8 Beam Dynamics: Vertical Waist Model

1. ω_a is senstive to the width of the beam, which is characterized by the frequency

$$f_{VW} = f_{cyc} - 2f_y, \tag{2.8}$$

$$f_y = f_{cbo} \sqrt{\frac{2f_{cyc}}{f_{cbo}} - 1}. \tag{2.9}$$

   In the 60H dataset $f_{VW} \approx 2.3\,\text{MHz} \approx 10 \cdot \omega_a$, an even multiple of the g-2 frequency. Because of this, the vertical waist largely cancels in the numerator of the ratio. (show this explicitly?) This combined with the time randomization to remove the fast rotation (f_{cyc}) means the vertical waist does not need to be included in the ratio fit. This is justified by the lack of a vertical waist peak in the FFT of the residuals of the fit. (mention at all how there is a very small but observable peak at very early times or omit it?)

2. If included, an exponential function is assumed for the VW decoherence as in the CBO, and the final VW term is

$$V(t) = 1 + A_{VW} e^{-t/\tau_{VW}} \cos(\omega_{VW} t + \phi_{VW}) \tag{2.10}$$

3. ω_{VW} is assumed to be a constant value even though the CBO frequency changes vs time.

2.9 Final Fit Function

The following function is used for the final fit for each calorimeter and for the calorimeter sum:

$$R(t) = \frac{2f(t) - f_+(t) - f_-(t)}{2f(t) + f_+(t) + f_-(t)} \tag{2.11}$$

$$f_\pm(t) = f(t \pm T_a/2) \tag{2.12}$$

$$f(t) = C(t)(1 + A\cos(\omega_a t + \phi)) \tag{2.13}$$

$$C(t) = 1 + A_{cbo} e^{-t/\tau_{cbo}} \cos(\omega_{cbo}(t)t + \phi_{cbo}) \tag{2.14}$$

$$\omega_a = 2\pi \cdot 0.2291\,\mathrm{MHz} \cdot (1 + R \times 10^{-6}) \tag{2.15}$$

All parameters are floating except for terms in $\omega_{cbo}(t)$ and τ_{cbo} as described above.

Chapter 3

Analysis Results

3.1 Pre-corrected and corrected energy and time spectra

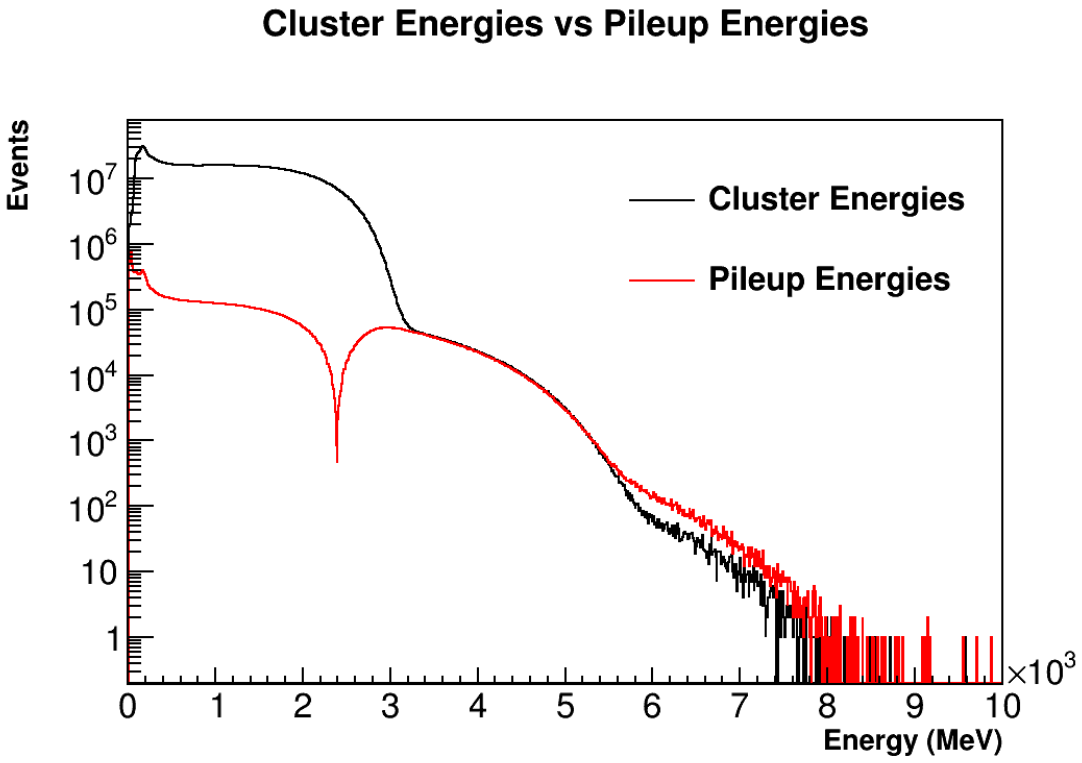

Figure 3·1: Cluster energies in black are plotted vs pileup energies in red, for all calorimeters added together. At energies below about 2.4 GeV the pileup spectrum goes negative. In this plot the absolute value of the pileup energies is plotted, and a spike at about 2.4 GeV can be seen as a consequence of this. Due to the triplets and contamination in the pileup spectrum, the red and black curves can be seen to diverge at high energies.

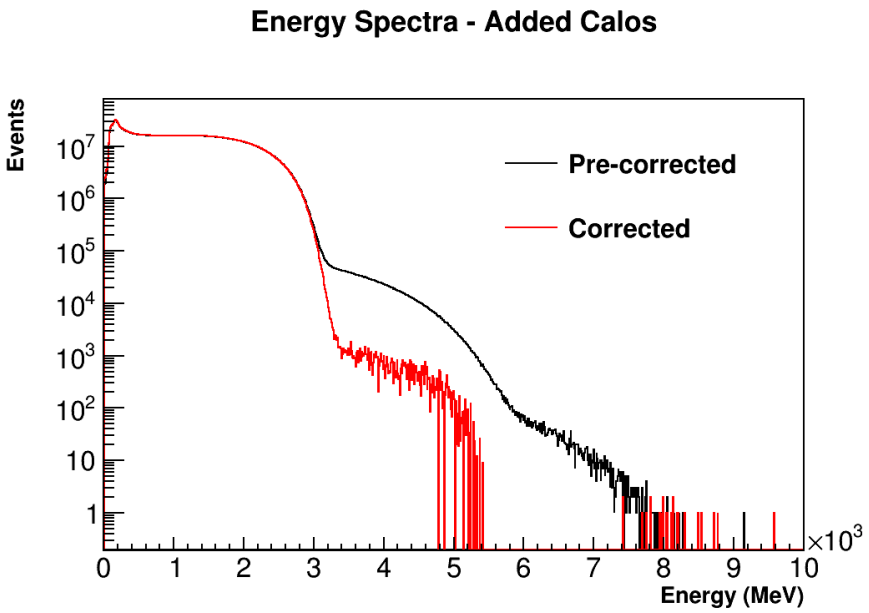

(a) Log scale - the corrected energy spectrum goes negative around 5 GeV.

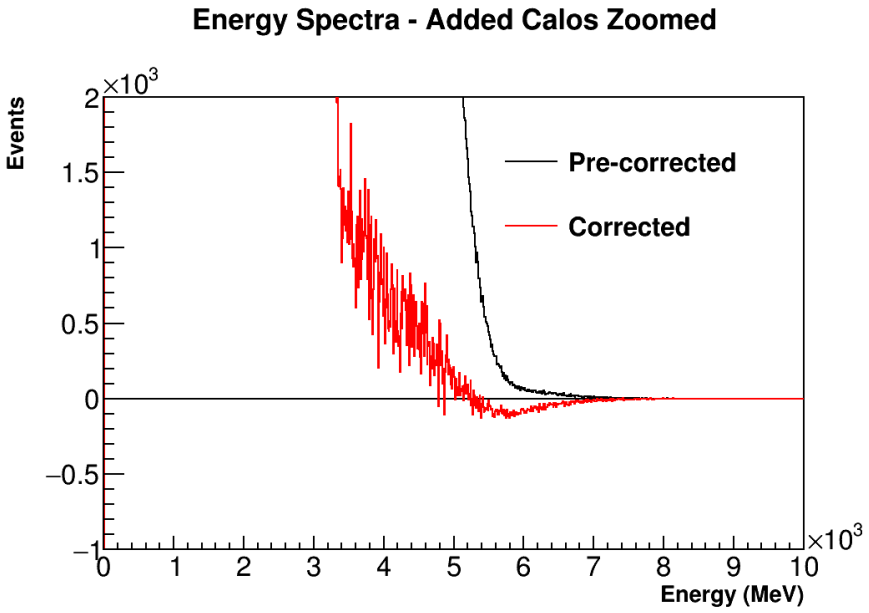

(b) Linear scale - zoomed in to show the shape.

Figure 3·2: Plots for the pre-corrected and corrected energy spectra are shown, all calorimeters added together. Because the triplets and contamination are not accounted for, the corrected energy spectrum does not lie exacltly along zero.

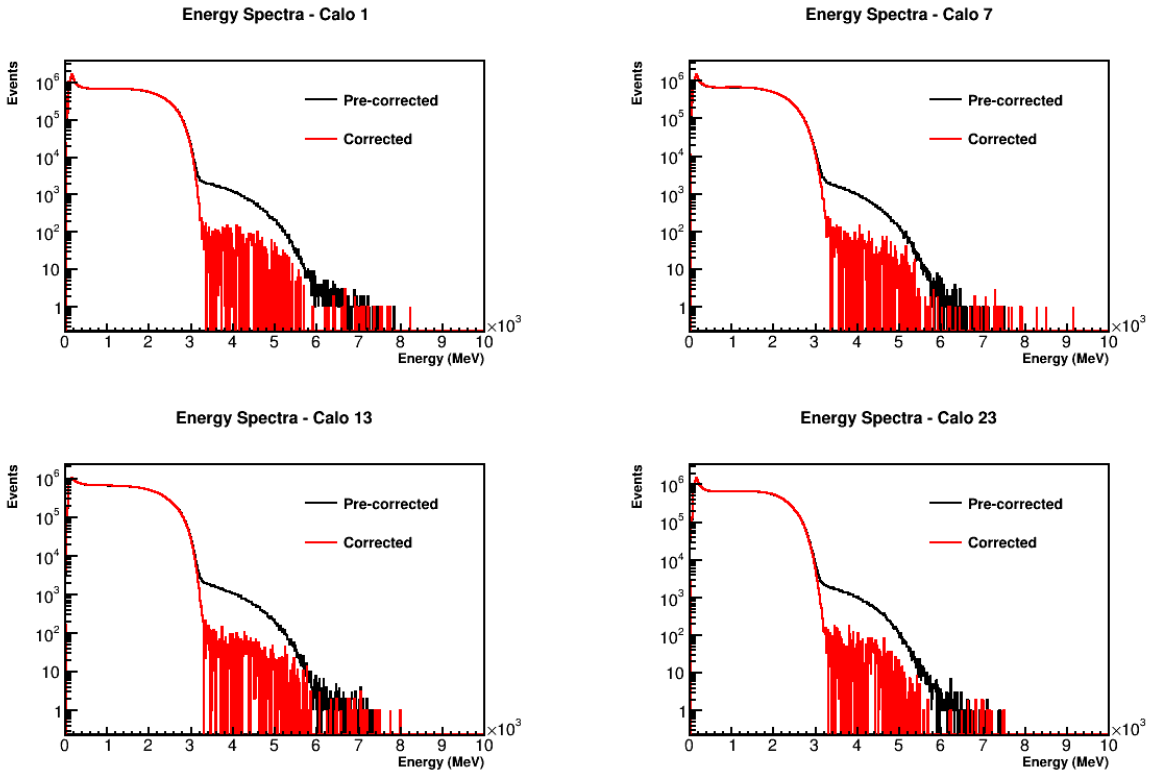

Figure 3·3: Pre-corrected and corrected energy spectra for calorimeters 1, 7, 13, and 23 plotted on a log scale.

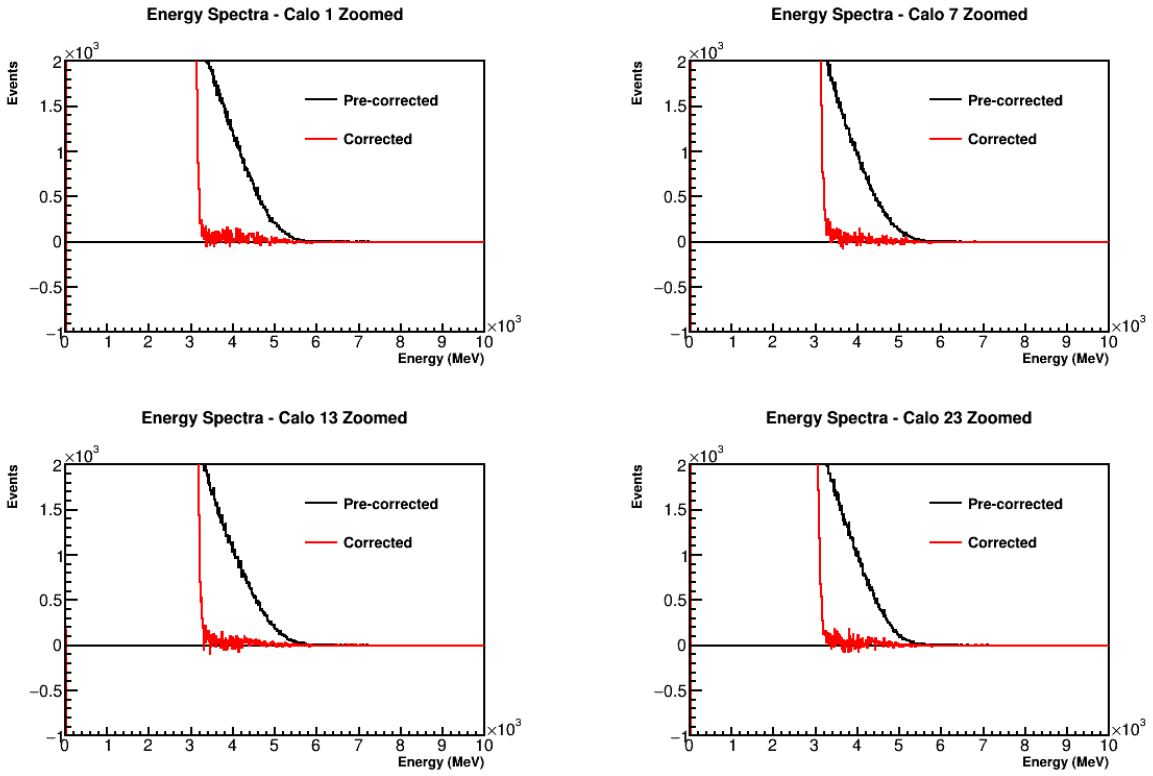

Figure 3·4: Pre-corrected and corrected energy spectra for calorimeters 1, 7, 13, and 23 plotted on a linear scale and zoomed in.

3.2 6 Parameter Ratio Fit

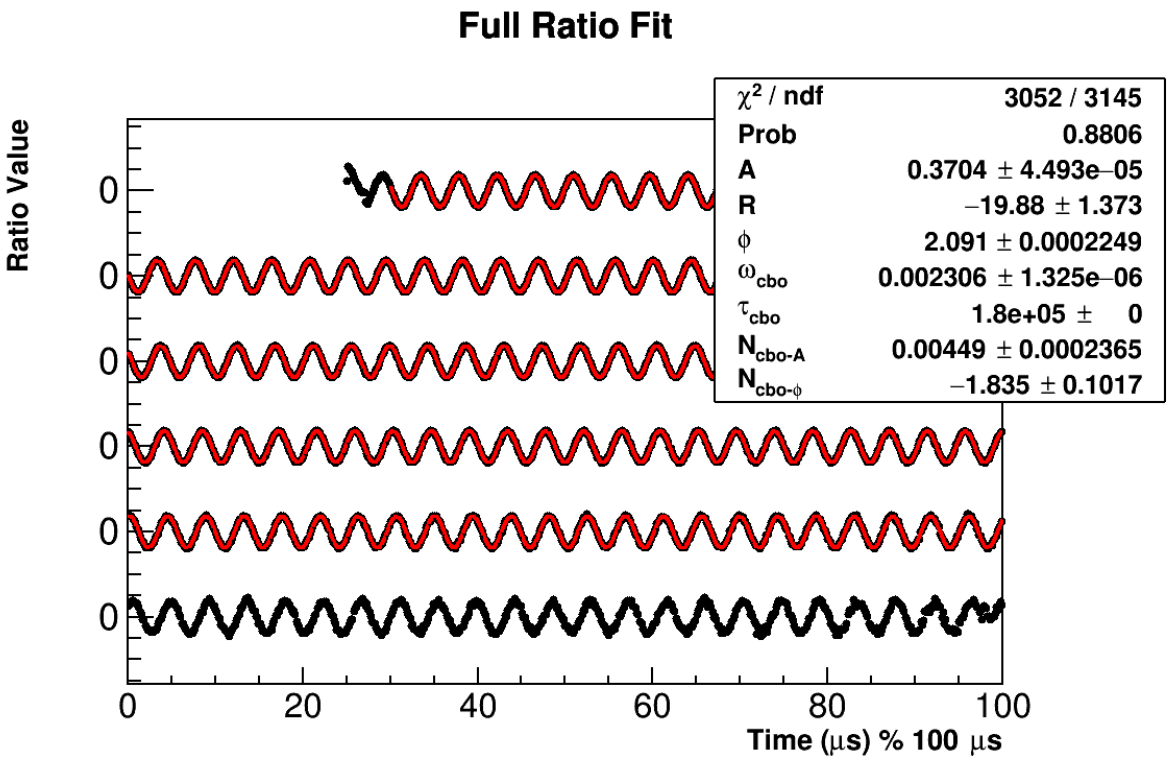

Figure 3·5: Final fit result for the 60 hour dataset. The fit includes 6 free parameters and one fixed. The x axis is in units of μs modulo 100 μs, with successive portions of the data points and fit shifted downwards on the plot. The parameter values in the stats box for the CBO frequency and lifetime are in units of ns. R is blinded locally. The fit ranges from 30 μs to 500 μs.

3.3 Residual and FFT

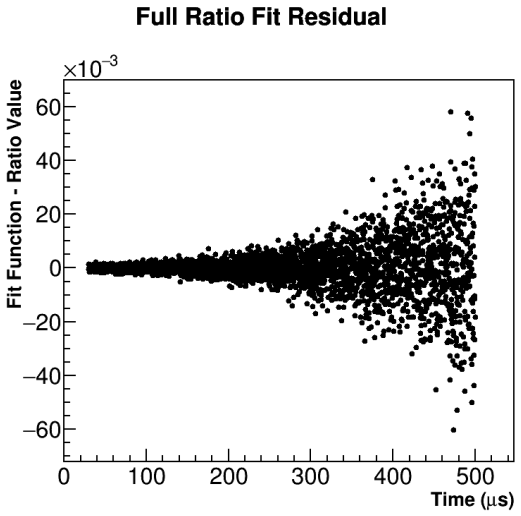

(a) Fit residuals.

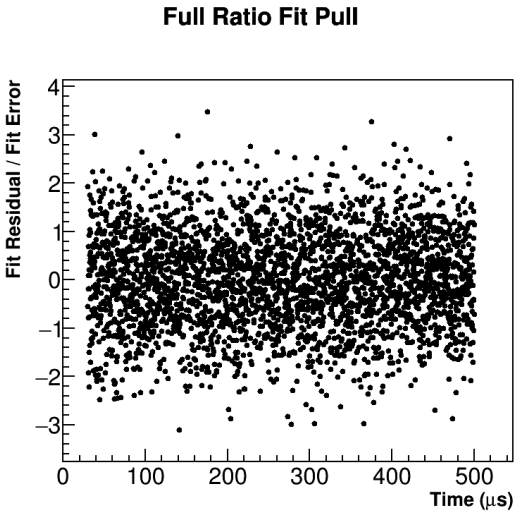

(b) Fit pulls.

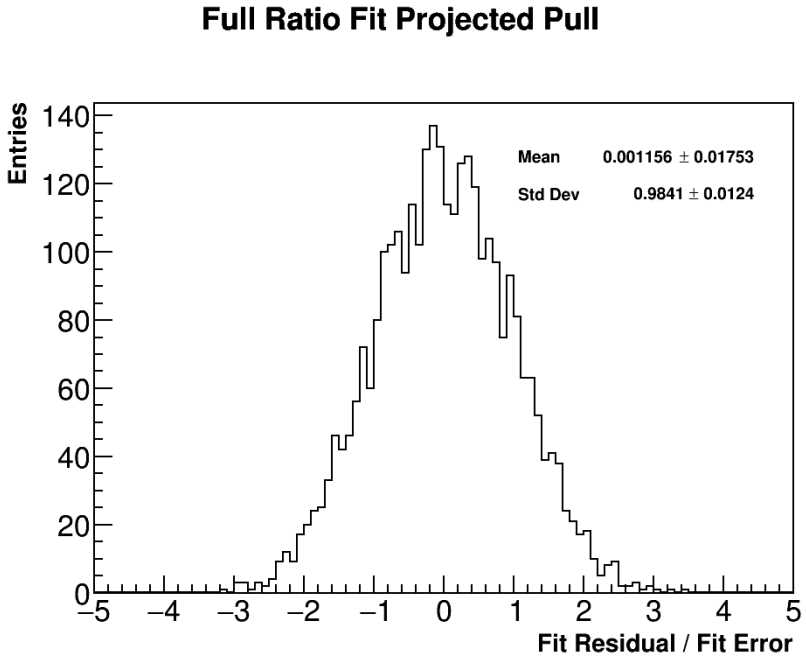

(c) Fit pulls projected onto the y axis. Note the Gaussian shape centered around 0 with unit width.

Figure 3·6: Residuals and pulls for the full ratio fit.

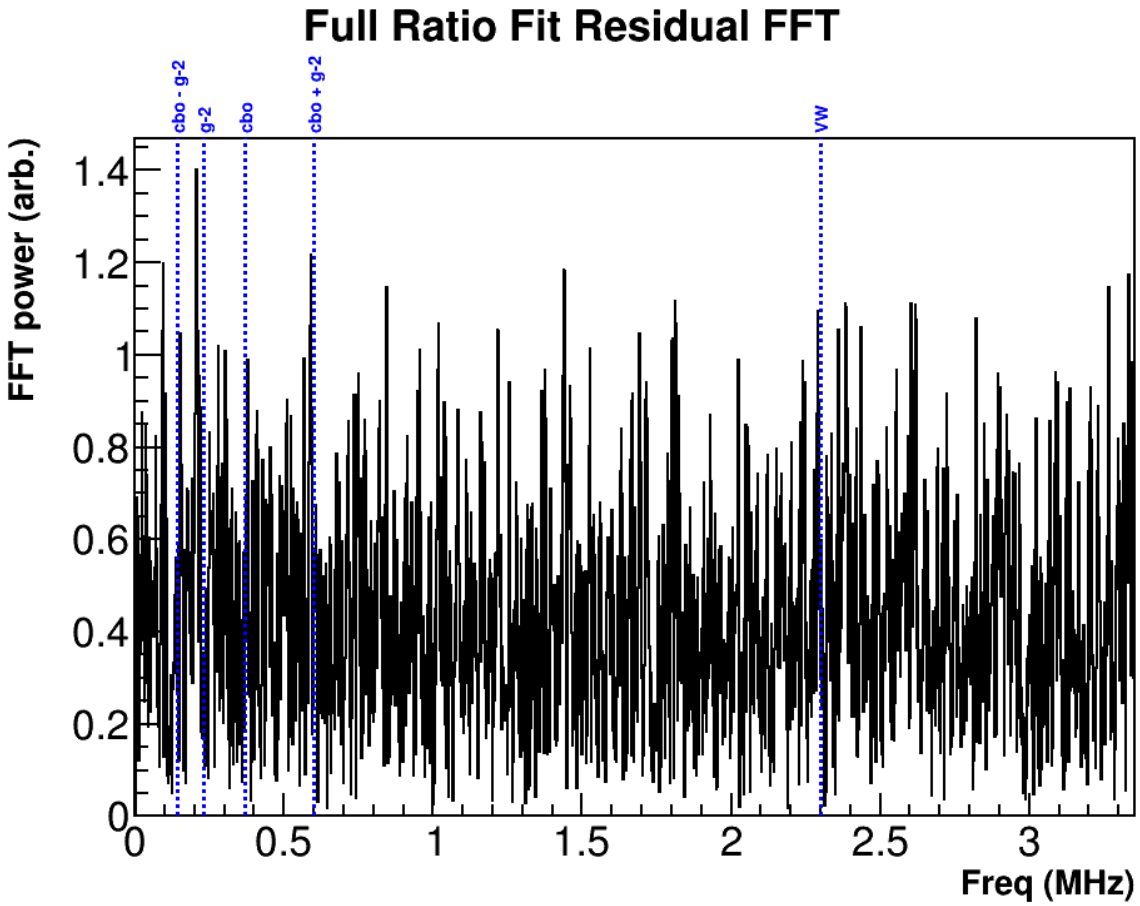

Figure 3·7: FFT of the residuals of the full ratio fit. No significant peaks remain in the ratio fit residuals after fitting with CBO terms. Overlayed are dotted lines for the $g-2$, CBO, and vertical waist frequencies. Peaks close to the lines are coincidental but don't line up when zoomed in.

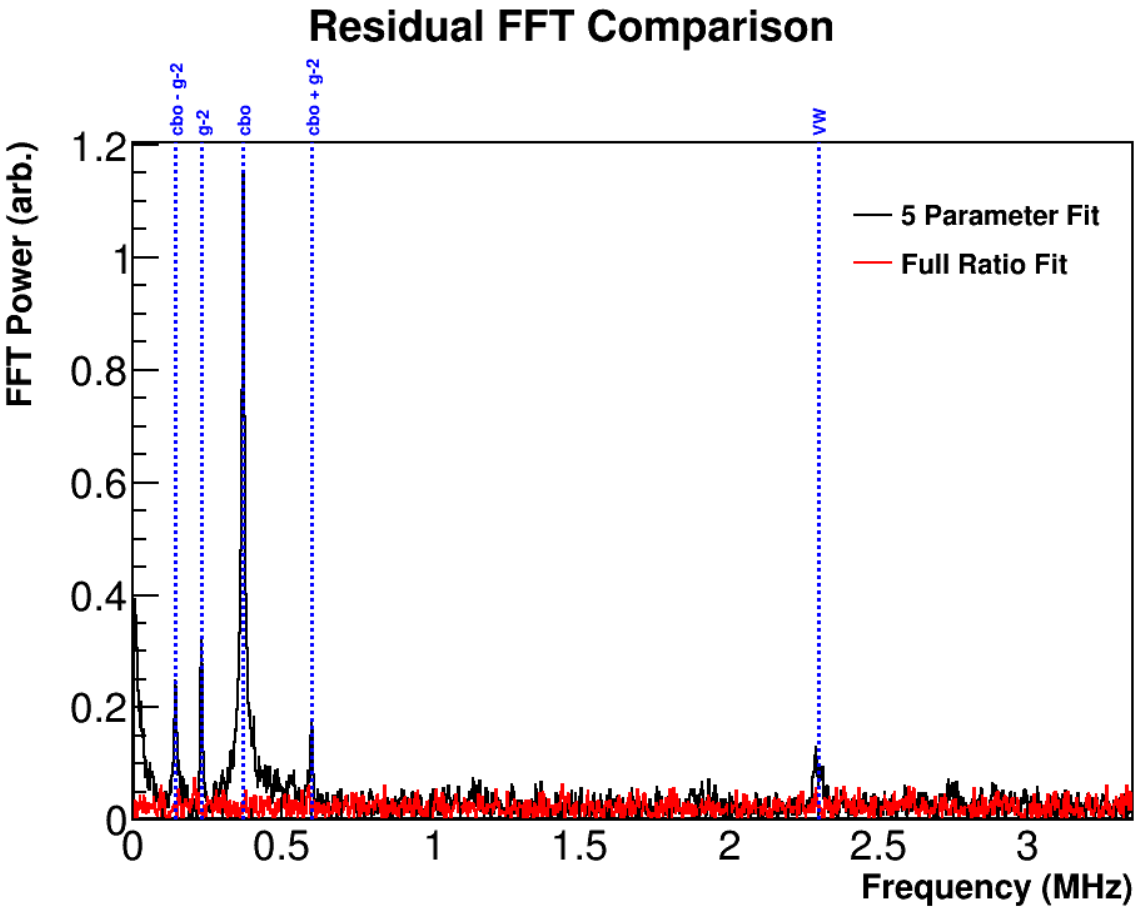

Figure 3·8: A plot of the FFT of the residuals of the fit for the five parameter fit compared to the ratio fit. In black is the FFT for a five parameter fit, where peaks for the CBO and vertical waist can be seen as well as the $g-2$ peak. In red is the FFT of the full ratio fit residuals, where it has been scaled up to be visible on this plot.

3.4 Start time scans

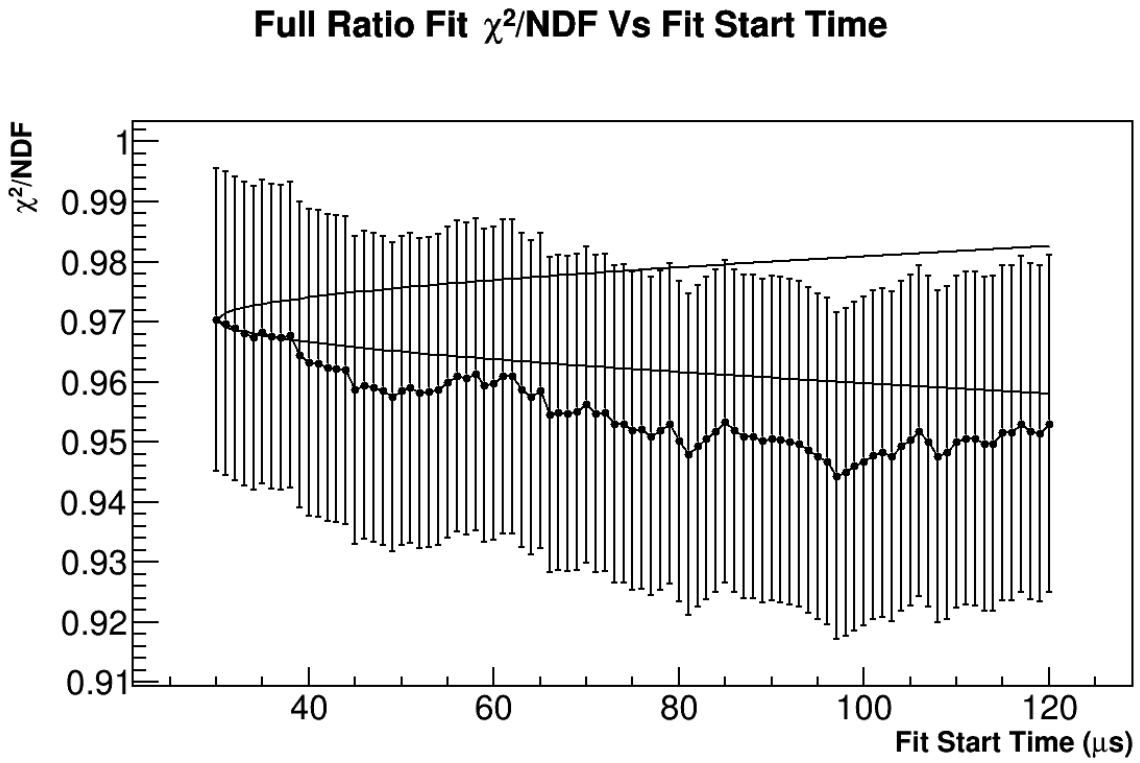

Figure 3·9: Plotted is the χ^2 per degree of freedom vs the start time of the fit. The solid lines indicate the one sigma statistically allowed difference in the fit result coming from the reduction in the data included in the fit. The error bars on the points are calculated as $\sqrt{2/NDF}$.

3.5 Stop time scans

I can produce stop time scans, and the results are consistent with the statistical significance bands, but some of the fits aren't perfect leading to some bad looking plots. Should I leave these out completely? Play more with the limits like I did to get the start time scans clean? Hack the plotting module to produce nicer looking plots? Or only include the good looking plots like R and the chi2?

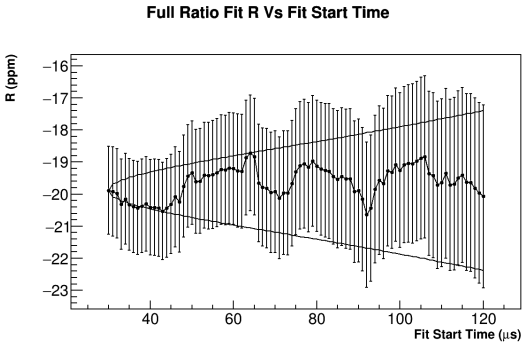

(a) Fitted R value vs fit start time.

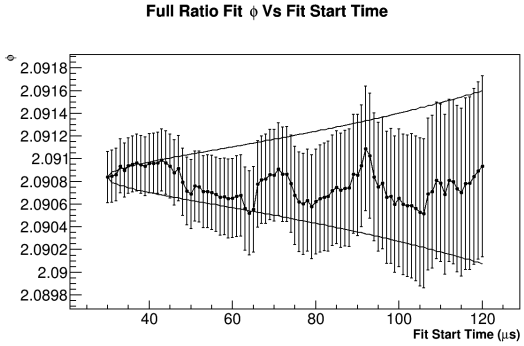

(b) Fitted $g-2$ phase vs fit start time.

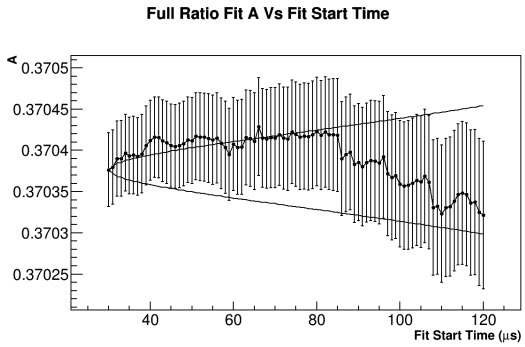

(c) Fitted asymmetry vs fit start time.

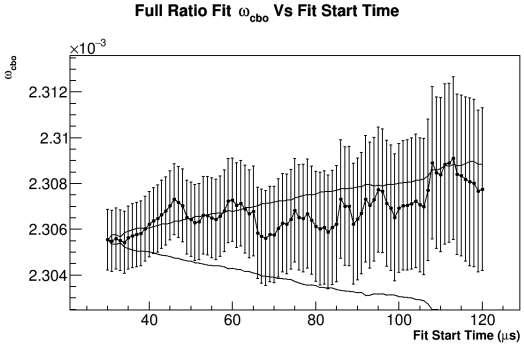

(d) Fitted CBO frequency (ω_0) vs fit start time.

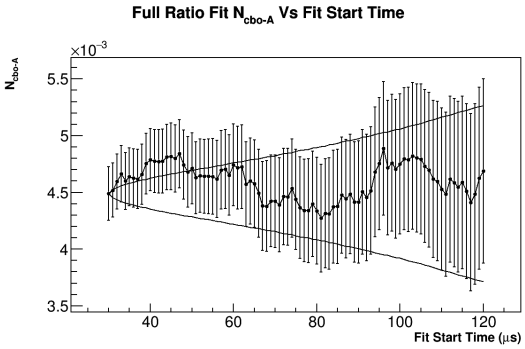

(e) Fitted CBO amplitdue vs fit start time.

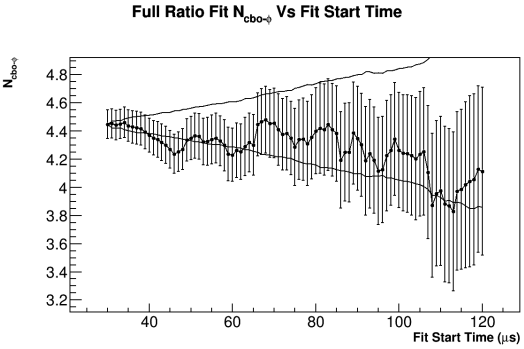

(f) Fitted CBO phase vs fit start time.

Figure 3·10: Start time scans for the free parameters in the full ratio fit. All parameters are consistently within the one sigma statistical bands.

3.6 Results vs calorimeter

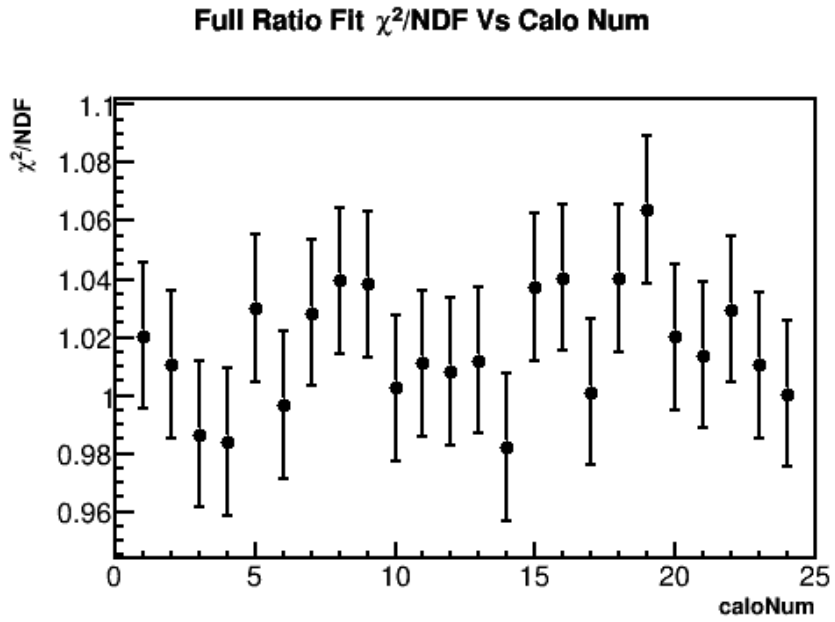

Figure 3·11: Plotted is the χ^2 per degree of freedom vs calorimeter number.

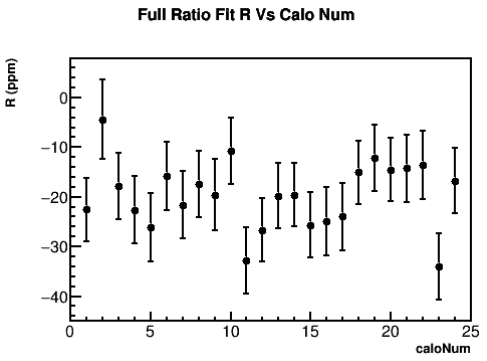

(a) Fitted R value vs calorimeter number.

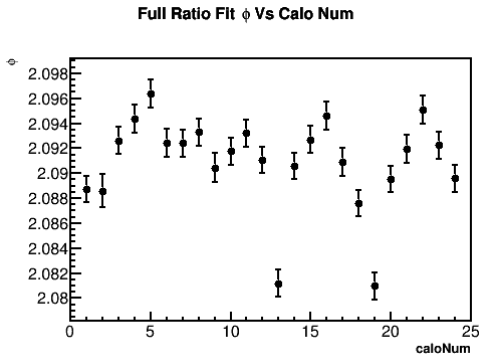

(b) Fitted $g-2$ phase vs calorimeter number. Calorimeters 13 and 19 lie behind the trackers leading to the different $g-2$ phases.

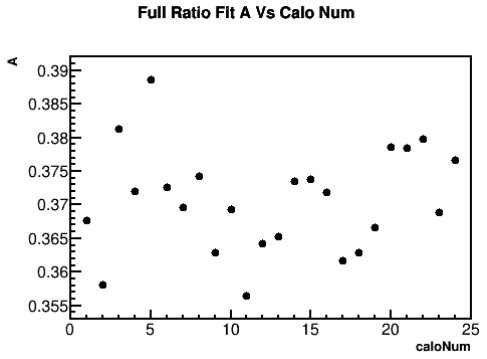

(c) Fitted asymmetry vs calorimeter number.

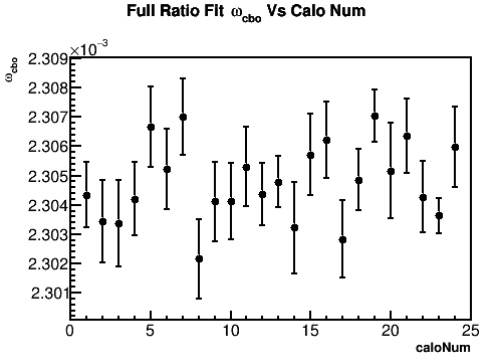

(d) Fitted CBO frequency (ω_0) vs calorimeter number.

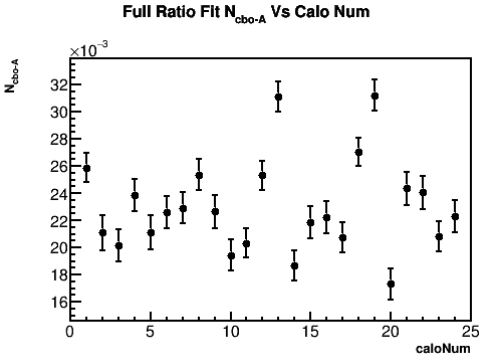

(e) Fitted CBO amplitdue vs calorimeter number.

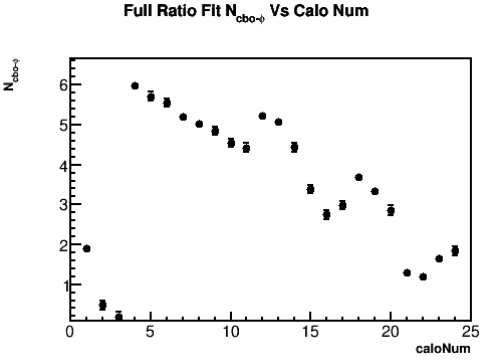

(f) Fitted CBO phase vs calorimeter number. The CBO phase varies from 0 to 2π around the ring.

Figure 3·12: Full ratio fit parameter values vs calorimeter number.

3.7 Correlation matrix for fit parameters

	A	R	ϕ	ω_{cbo}	τ_{cbo} (fixed)	N_{cbo-A}	$N_{cbo-\phi}$
A	1.0000	**0.0049**	−0.0068	−0.0166	0.0000	−0.0098	0.0233
R	0.0049	**1.0000**	−0.8300	−0.0204	0.0000	0.0207	0.0282
ϕ	−0.0068	**−0.8300**	1.0000	0.0280	0.0000	−0.0287	−0.0387
ω_{cbo}	−0.0166	**−0.0204**	0.0280	1.0000	0.0000	0.0773	−0.8585
τ_{cbo} (fixed)	0.0000	**0.0000**	0.0000	0.0000	1.0000	0.0000	0.0000
N_{cbo-A}	−0.0098	**0.0207**	−0.0287	0.0773	0.0000	1.0000	−0.0656
$N_{cbo-\phi}$	0.0233	**0.0282**	−0.0387	−0.8585	0.0000	−0.0656	1.0000

Table 3.1: Correlation matrix for the full ratio fit. The CBO lifetime is fixed but included in this table. The only significant correlation to R is the $g-2$ phase.

Chapter 4

Systematic Uncertainty Evaluations

4.1 Sensitivity of ω_a to gain corrections

4.1.1 In-Fill Gain

As positrons hit the calorimeters throughout the fill, there will be a gain sag response such that the energy of detected positrons changes throughout the fill, dropping at first and then rising exponentially back up to their true values. This changing energy response will lead to a systematic error on R, as positrons with mis-measured energies near the energy threshold are excluded from the fit. This gain sag is corrected for in the Recon West code, before I fill my histograms. Due to the way I've constructed my analysis code, it's not so simple to modify the reconstruction code and create new histograms quickly. Such a process would require the rebuilding of many sets of new cluster root trees, and then making histograms from those. As a faster way of getting at the in fill gain systematic error, I've instead chosen to apply a gain sag function to the incoming energy-corrected clusters. This allows me to scan over gain sag function parameters and only run off one set of trees, as I've been doing for all systematic studies.

(Should this bit be in the analysis procedures chapter?) The in-fill gain sag function was determined by Matthias Smith and the laser team as shown in DocDB 14077. (Cite or link?) The function goes as

$$E = E_0(1 - A \cdot e^{-(t-t_{offset})/\tau}), \tag{4.1}$$

where E_0 is the orginal energy of the positron cluster, A is the amplitude factor on the gain sag function, τ the lifetime, and then t_{offset} the shift of the function from 0. It is this function that is inverted and applied to the clusters in the reconstruction. I apply a function of the same form in my own code before filling hits into histograms, in essence undoing the reconstruction gain correction as a way to measure the in-fill gain sag effect on R.

There are some simplifications and assumptions I've made when applying said gain sag function in my own code. First is that while in the reconstruction code each crystal of each calorimeter has its own singular in-fill gain function, one of which is shown in Figure 4·1, I apply a global gain sag function to all incoming clusters. Secondly the default parameters for the gain sag function are simply eyeballed from the fcl file where all crystal parameters are stored. These values are 0.03 for the amplitude, 6.7 μs for the lifetime, and 3.907 μs for the offset. (Once the latest dataset is available I will need to come up with a better way to apply this gain sag function, either with multiple functions per crystal or with parameters that are actual averages. For now it's fine though to get words on the paper.) Finally, I apply this gain sag function after I apply the artificial deadtime to the incoming clusters,

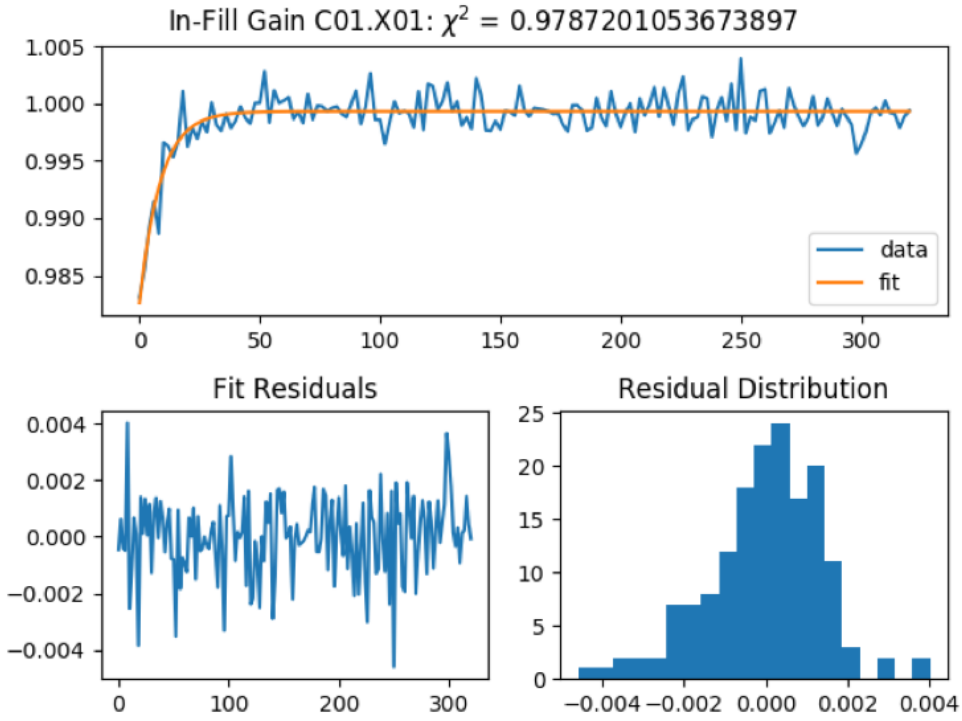

Figure 4·1: The top plot shows the in-fill gain sag function in orange from a fit to data in blue, for crystal 1 in calorimeter 1. The gain sag can be modeled effectively by a simple exponential function. By 30 μs the change in energy response is nearly only .1%. (Might want to look up these exact numbers.) The bottom two plots show the residuals of the fit. Plot made by Matthias Smith.

due to code restrictions. This should be a small effect. These assumptions I believe should be okay as long as I take my systematic errors conservatively.

To calculate the systematic error, I simply scan over the gain sag function parameters and observe the changes in R. This includes scans over the amplitude, lifetime, and offset as described in 4.1, and shown in Figure 4·2. I calculate the systematic error on R as the quadrature sum of the separate pieces as

$$\delta R_A = \delta\alpha_A \times \frac{dR}{d\alpha_A}, \tag{4.2}$$

$$\delta R_\tau = \delta\alpha_\tau \times \frac{dR}{d\alpha_\tau}, \tag{4.3}$$

$$\delta R_{offset} = \delta\alpha_{offset} \times \frac{dR}{d\alpha_{offset}}, \tag{4.4}$$

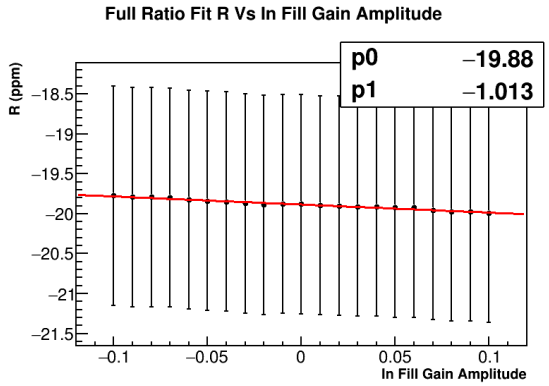

(a) Plotted is R vs the amplitude parameter in the gain sag function. The slope is -1.013 ppm per unit amplitude.

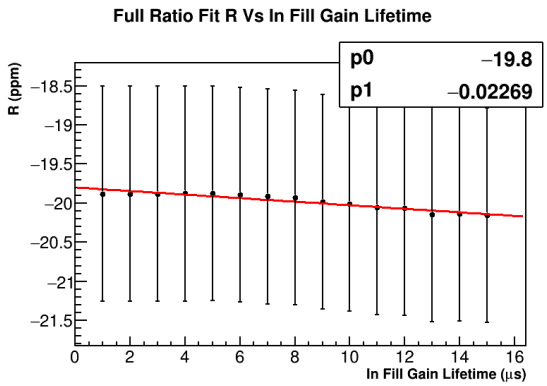

(b) Plotted is R vs the lifetime parameter in the gain sag function. The slope is -0.02269 ppm per μs.

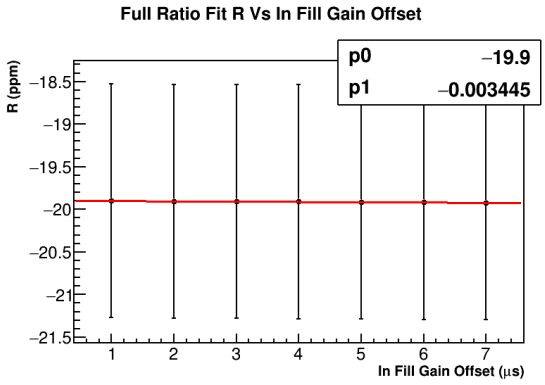

(c) Plotted is R vs the offset parameter in the gain sag function. The slope is -0.0034 ppm per μs.

Figure 4·2: Plotted is fitted R values vs gain sag function parameters. In each case I scanned over ranges approximately centered around the eyeballed average values.

where $\delta\alpha_A$, $\delta\alpha_\tau$, and $\delta\alpha_{offset}$ are the uncertainties on the gain sag amplitude, lifetime, and offset respectively. I take the uncertainty on the amplitude very conservatively at 1%, leading to a systematic error on R of $0.01 \times 1.013\,\text{ppm} = 10.1\,\text{ppb}$. I take the uncertainty on the lifetime very conservatively at $1\,\mu$s, leading to a systematic error on R of $1 \times 22.7\,\text{ppb} = 22.7\,\text{ppb}$. Finally the slope for the offset parameter is very flat, and that combined with a very uniform array of values for the offset parameter in the reconstruction (indicative of a very small uncertainty), means that the systematic error on R is negligible. Therefore I ignore the offset parameter and add the amplitude and lifetime errors in quadrature to produce a systematic error on R of 24.8 ppb. (The uncertainty on the parameters would be the fit errors on the parameter I think, except for the fact that I'm using a global gain sag function as opposed to crystal functions, meaning the uncertainty might be the spread in parameters. I'm not entirely sure. Maybe ask Matthias/Laser team and James.)

4.1.2 Short Term Double Pulse (SDTP)

4.2 Sensitivity of ω_a to pileup

The systematic error on R due to the pileup construction consists primarily of two parts, the error due to misconstruction of the amplitude and the phase of the pileup.

4.2.1 Pileup Amplitude

The error due to the amplitude misconstruction was calculated by scanning over a pileup multiplier parameter, from 90% of the calculated pileup amplitude to 110%, as shown in Figure 4·3. The sensitivity of R to the amplitude was determined to be 509.1 ppb per unit amplitude. The uncertainty of the pileup amplitude construction was determined by fitting a parabola to the χ^2 as a function of the pileup amplitude, and taking the width of that parabola as the uncertainty. This width is determined as the distance in X for the χ^2 to rise by 1 from the minimum, also calculated as $\sqrt{2/(\chi^2)''}$.

This corresponds to an uncertainty of $\sqrt{1/508.4} = 0.0444$ or 4.44%. The minimum of the χ^2 plot of 1.022 lies at approximately $.5\sigma$ away from 1, which is consistent and nice to see. Then, calculating the systematic error on R due to the pileup amplitude construction as

$$\delta R_{pm} = \delta\alpha_{pm} \times \frac{dR}{d\alpha_{pm}} \tag{4.5}$$

where $\delta\alpha_{pm}$ is the uncertainty on the pileup amplitude, the systematic error on R is calculated as $0.0444 \times 509.1\,\text{ppb} = 22.6\,\text{ppb}$.

Another technique to estimate the uncertainty of the pileup amplitude construction is

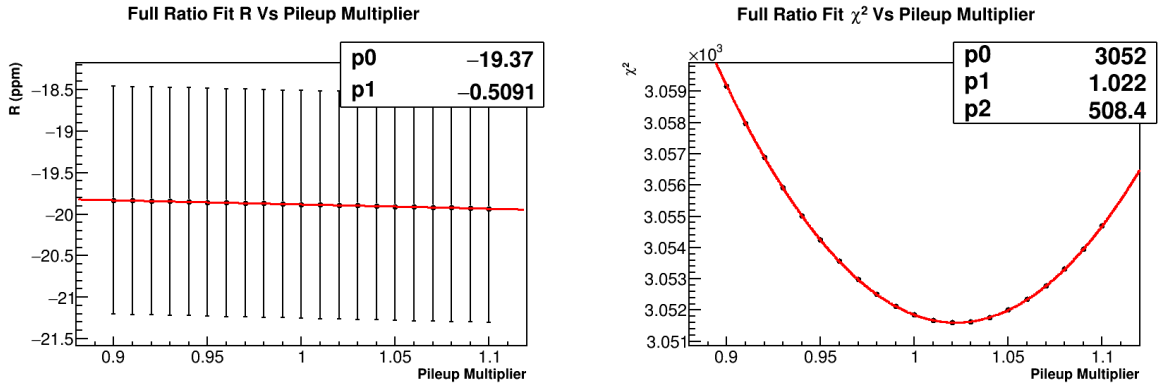

(a) Sensitivity of R vs the pileup amplitude. The slope is -509.1 ppb per unit amplitude.

(b) Plotted is the fitted χ^2 vs the pileup amplitude. The fit equation used was $p2 \times (x - p1)^2 + p0$. The minimum therefore lies at 1.022.

Figure 4·3: The significant plots to determine the pileup amplitude systematic error.

to look at the offset of the high energy tail of the pileup subtracted energy spectrum from zero. Because however I've applied only the doublet correction, I know that the shape of the pileup spectrum is wrong by some amount, as evidenced in Figure 3·2. While the pileup itself can multiplied by some scaling factor other than 1 in order to align the energy spectra slightly better, because the shape of the pileup correction is imperfect the offset calculation I believe is the wrong way to go about calculating this uncertainty in my case. The shape can be fixed by including the triplets and the doublet contamination in the shadow method, but that work is incomplete. Since the triplets are a 1% effect relative to the doublets, and the contamination is of the same order, I believe the uncertainty of 4.44% conservatively includes for this mismatch in shape and the omission of the triplets. Regardless, since the statistics of the 60H dataset is much larger than the order of the systematic effect for the pileup construction ($\mathcal{O}$(1 ppm) vs $\mathcal{O}$(10 ppb)), this is a fine assumption.

4.2.2 Pileup Phase

The error on R due to the pileup phase construction was calculated by scanning over a pileup time shift parameter, where the pileup spectrum was shifted in time by some amount before subtraction. The sensitivity of R to this parameter is shown in Figure 4·4. It is extremely unlikely that the entire pileup spectrum could be shifted by the offsets shown here, so this is a conservative estimate of the effect of the pileup phase on R. I then calculate the phase

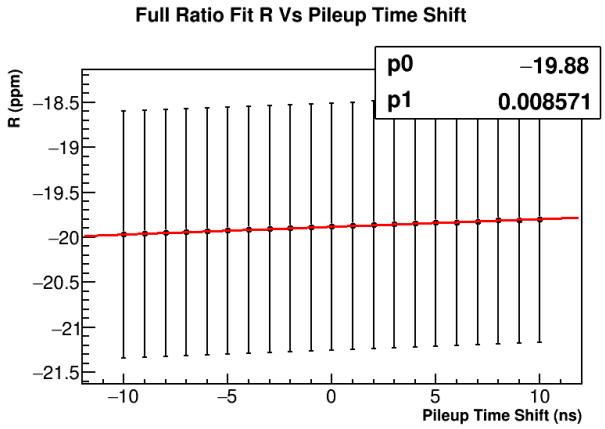

Figure 4·4: Sensitivity of R vs the pileup phase. The slope is 8.571 ppb per ns.

error as

$$\delta R_{pp} = \delta\alpha_{pp} \times \frac{dR}{d\alpha_{pp}} \tag{4.6}$$

where $\delta\alpha_{pp}$ is the uncertainty on the pileup phase. I once again very conservatively estimate the uncertainty on the pileup phase as half the artificial deadtime at 3 ns. The systematic error on R is then calculated as $3\,\text{ns} \times 8.571\,\text{ppb/ns} = 25.7\,\text{ppb}$. This is a very conservative estimate which is fine once again because of the comparison of order of statistics vs the systematic effect.

// reference the figure below

// change text and include new plots

Another factor that the phase depends on is the energy dependence of the constructed pileup pulses, calculated as just the sum of the singlets. If the energy is miscalculated then the phase of the included pulses will be off. However, because the spatial separation is turned off in the reconstruction clustering, this is a small effect for my pileup construction method. Similarly, in the near future the Short Term Double Pulse (STDP) improvement to the laser calibration will be included also reducing this effect. For these reasons and due to the conservative nature of my phase error estimation, I leave such effects out.

Adding these two errors in quadrature results in a systematic error on R due to the pileup as 34.2 ppb.

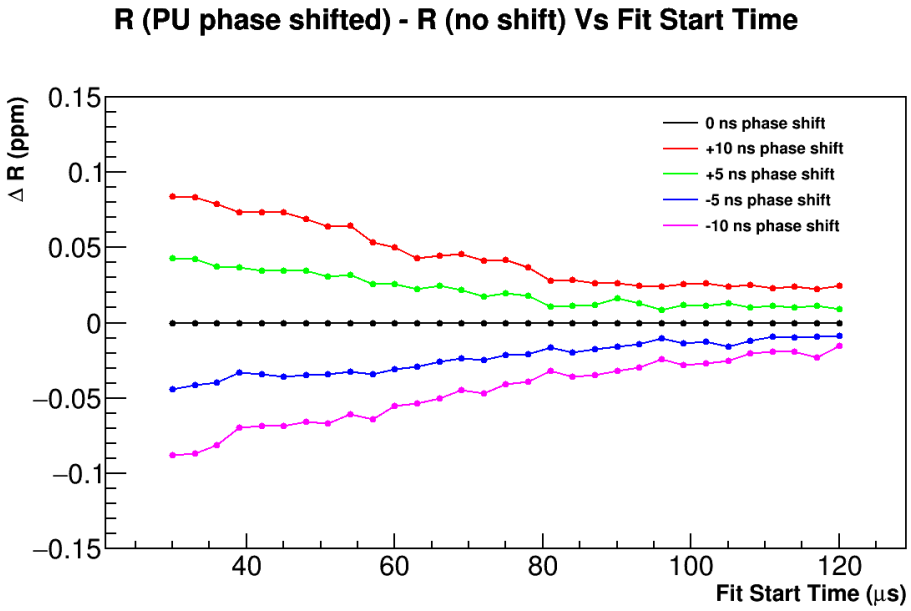

Figure 4·5: Plotted is ΔR between pileup time shifted and unshifted results vs fit start time. The black line and points are by definition 0. As the fit start time increases and the pileup reduces, the ΔR points converge to zero as they should.

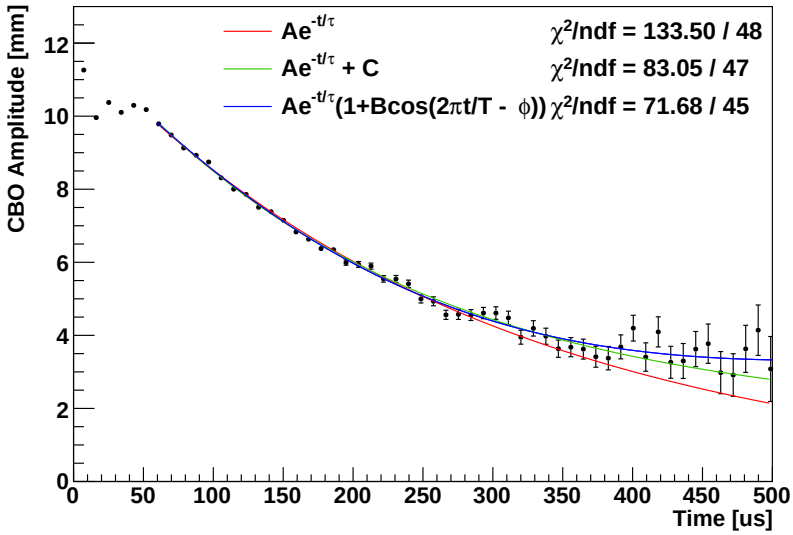

Figure 4·6: Plotted is the CBO amplitude as a function of time from the tracker analysis. Three separate fit functions were used with varying degrees of success to characterize the envelope shape of the CBO (excepting the cosine modulation part). A Gaussian fit was tried with no success. The amplitude isn't fully understood at early times. The period $T/2\pi$ has a value of 114.5 μs. Plot producd by James Mott.

4.3 Sensitivity of ω_a to lost muon function shape

4.4 Sensitivity of ω_a to CBO function

4.4.1 CBO Shape

If the shape of the CBO in the fit function is wrong, then there will be a systematic error on R. Because I get good fits and the CBO parameters are stable vs fit start time, the possbile changes to the envelope are limited, compared to the envelope used as shown in Equation 2.7. Possible changes to the envelope include those functions as shown in Figure 4·6, an exponential plus a constant and then an exponential times another oscillatory term. Both new envelopes were determined from tracker analysis fits to the CBO amplitude. Both changes to the envelope amplitude were tried in the fitting function, with changes in R of -21.1 ppb and -9.6 ppb respectively, though neither showed any improvement in the fit. (In the latter the period of the oscillatory term was fixed and the other parameters were allowed to float.) I take the latter value of 21.1 ppb as the systematic error on R due to the shape.

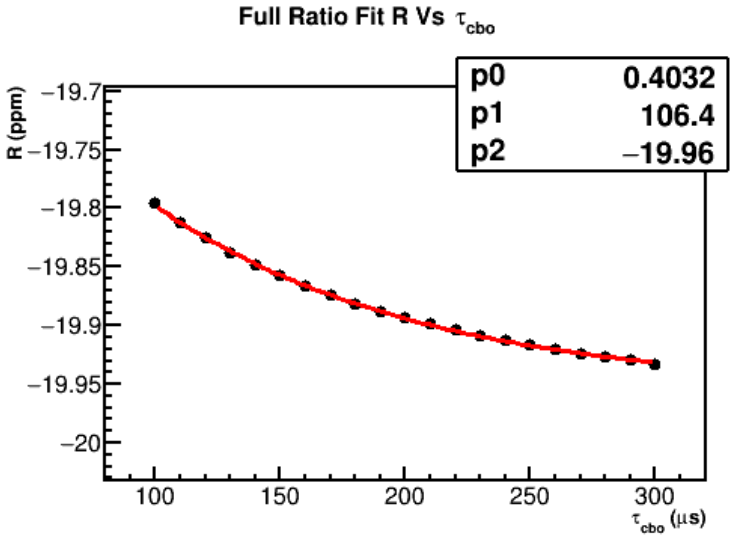

Figure 4·7: Plotted is the fitted R value as a function of the CBO lifetime, which has been fixed in the full ratio fit. The error bars have been removed from the plot in order to show the shape of the curve better. The points have been fitted to an exponential function which lines up nicely, $p_0 e^{-t/p_1} + p_2$.

4.4.2 CBO Frequency

What about systematic errors for the cbo frequency? Should this be provided from the trackers or something that I do?

4.4.3 CBO Lifetime

Because the CBO lifetime has been fixed in the fit, there is a systematic error on R. Scanning over various values of the fixed CBO lifetime allows this error to be calculated. The resulting curve of R vs the CBO lifetime turns out not to be linear, as shown in Figure 4·7. Taking the uncertainty on the CBO lifetime as the error produced by the T Method fit, approximately 16 μs, and looking at the change in R for CBO lifetime values of $180 \pm 16\,\mu$s, the systematic error on R is taken as the larger of the two at 12.1 ppb.

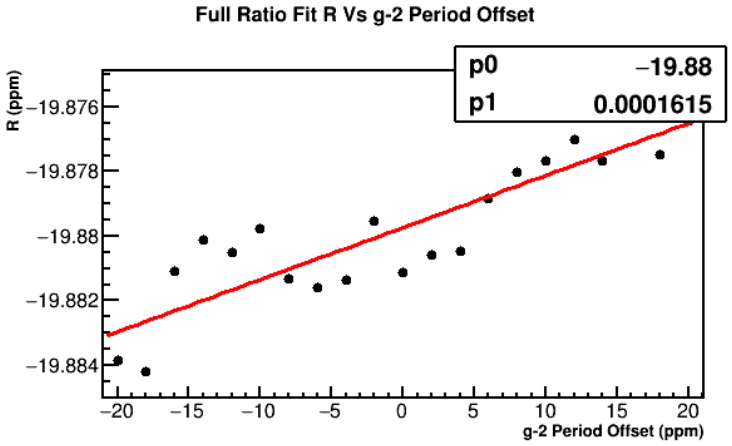

Figure 4·8: Fitted R value as a function of the ppm level offset from the guess used for the $g-2$ period, 2.1. Error bars have been removed from this plot, otherwise it appears as a flat line. The slope is .16 ppb per ppm offset in T_a.

4.5 Sensitivity of ω_a to VW function

4.6 Sensitivity of ω_a to various effects

4.6.1 $g-2$ Period Guess

To perform the ratio method, the $g-2$ period needs to be known a priori to high precision. By scanning over various $g-2$ period guesses the dependence of R on T_a can be determined, as shown in Figure 4·8. The systematic error can then be calculated as

$$\delta R_{period} = \delta\alpha_{period} \times \frac{dR}{d\alpha_{period}} \tag{4.7}$$

where $\delta\alpha_{period}$ is the uncertainty on T_a. Very conservatively taking the uncertainty as 10 ppm, the systematic error on R is calcualted as $10\,\text{ppm} \times 1.62 \times 10^{-4}\,\text{ppm/ppm} = 1.62\,\text{ppb}$, which is completely negligible.

4.6.2 Bin Width

The systematic uncertainty from the bin width, chosen to eliminate the fast rotation signal, was calculated by performing the histogramming and fitting stages with varying values of bin widths. The systematic uncertainty is taken as the RMS spread of the fitted R values. As shown in Figure 4·9 it is 44.5 ppb.

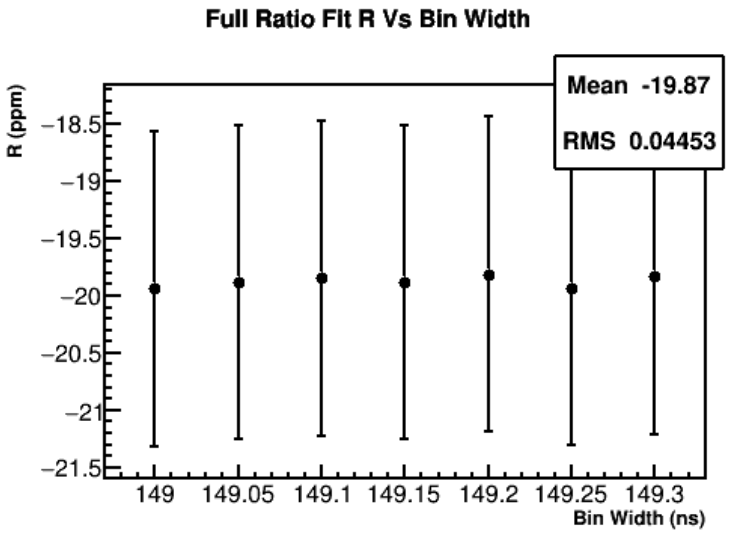

Figure 4·9: Plotted are fitted R values for varying bin widths ranging from 149.00 ns to 149.30 ns in steps of 5 ns.

4.6.3 Randomization

In the histogramming phase of my analysis, random seeds are used in two places. One for the randomization of counts into the 4 separate datasets that go into the ratio, and one for the time randomization to reduce the fast rotation. It's necessary to make sure that results are consistent among random seeds, and that the final answer wasn't a particularly fortuitous or disastrous choice. In order to test this I performed fits with 20 different random seeds, the χ^2/NDF and fitted R values of which are plotted in Figure 4·10. Results are consistent and very much within error of each other. I also performed fit start scans for a couple of the random seeds as an extra check to make sure the fitting was behaving consistently as shown in Figure 4·11.

I'm not so sure there should be a systematic error on R due to the randomization. Such an error should be contained within the statistical error of the final answer I believe. However I calculate one here for posterity in the manner that was done for E821,

$$\delta R_{rand} = \sigma(R)/\sqrt{NDF}, \tag{4.8}$$

where $\sigma(R)$ is the RMS spread in R and NDF is the number of degrees of freedom which is equal to the number of random seeds minus one, in this case 19. Therefore with an RMS on R of 193.6 ppb, the systematic error on R due to the randomization is (potentially) 44.4 ppb. (The fact that simply increasing the number of seeds allows for this systematic error to reduce to zero as shown in Equation 4.8 gives greater weight to the argument that this

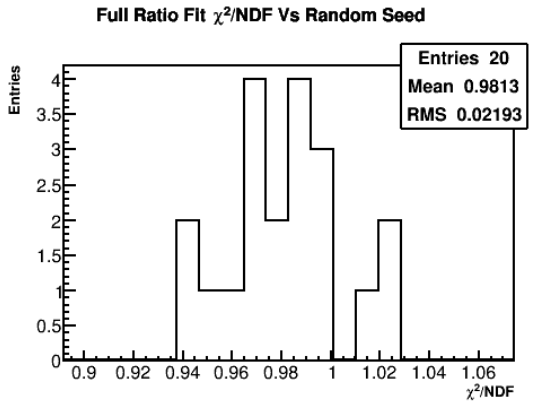

(a) χ^2/NDF values for 20 random seeds.

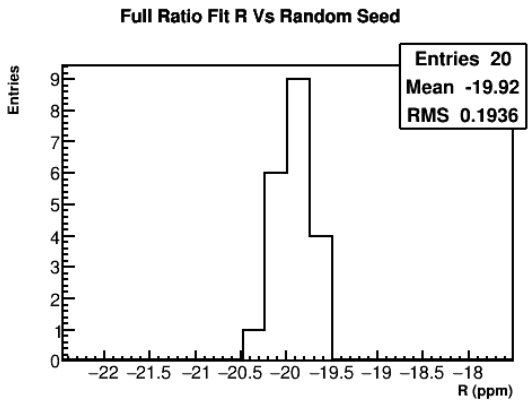

(b) R values for 20 random seeds.

Figure 4·10: Plotted is the χ^2/NDF and fitted R value for 20 random seeds.

really shouldn't be a systematic error at all, and is instead a purely statistical effect already taken care of in the fit.)

4.7 Final Systematic Uncertainty Table

Summary of Systematic Errors	
Systematic Error	60 H
Gain(+)	24.8
Pileup	34.2
Lost Muons	
CBO(+)	24.3
VW	
Bin Width	44.5
Randomization(?)	44.4
Other	
Total	

Table 4.1: Systematic error table for the 60H dataset. All units are in ppb.

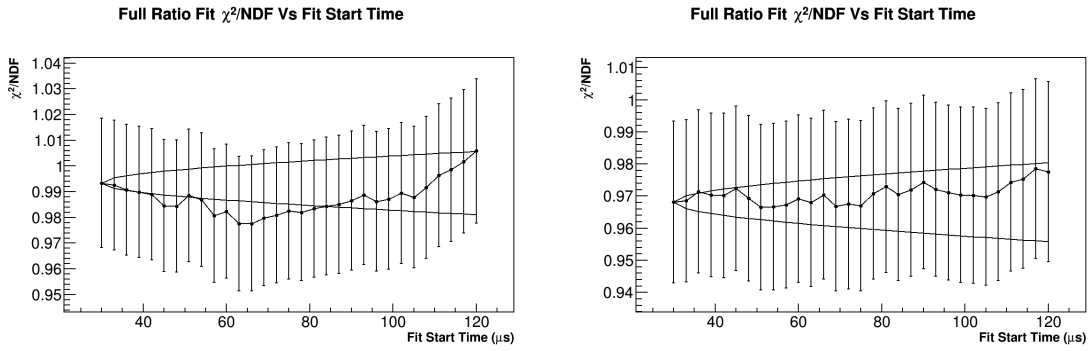

(a) Seed 1

(b) Seed 2

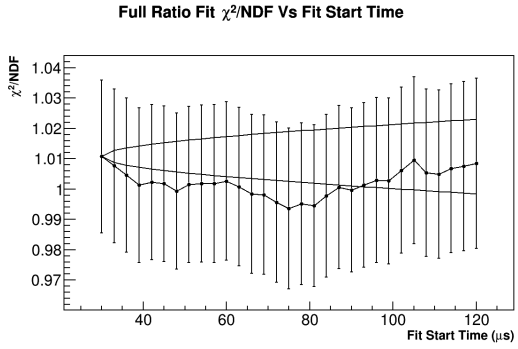

(c) Seed 3

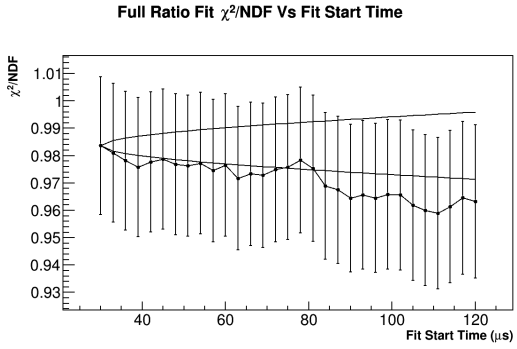

(d) Seed 4

Figure 4·11: Fit start time scans for the χ^2 for four random seeds of the randomization of the same dataset. Compare to Figure 3·9. The general behaviour of the fits vs fit start time is consistent and relatively the same, but as is seen the scans can rise and fall at different points due to the choice of randomization.

Chapter 5

Conclusion and Final Results

- $R = -19.88 \pm 1.373\,\text{ppm} \pm syst.$ (blinding with common string)
- $\chi^2/NDF = 3052/3145$

Appendix A

Ratio Method Derivation and Fit Function

Consider the 5 parameter function:

$$N_5(t) = N_0 e^{-t/\tau}(1 + A\cos(\omega_a t + \phi)), \tag{A.1}$$

which describes some ideal dataset in histogram format. Here ϕ will be set to zero for simplicity. Now define the variables $u_+(t)$, $u_-(t)$, $v_1(t)$, and $v_2(t)$ as

$$\begin{aligned} u_+(t) &= \frac{1}{4}N_5(t + T/2) \\ u_-(t) &= \frac{1}{4}N_5(t - T/2) \\ v_1(t) &= \frac{1}{4}N_5(t) \\ v_2(t) &= \frac{1}{4}N_5(t), \end{aligned} \tag{A.2}$$

where the 1/4 out front reflects randomly splitting the whole dataset into 4 equally weighted sub-datasets, and T is the g-2 period known to high precision, $\mathcal{O}(10^{-6})$. This corresponds to a weighting of 1:1:1:1 between the datasets. To be explicit here regarding the signs, the counts that are filled into the histogram described by u_+ have their times shifted as $t \to t - T/2$, which is what the function $N_5(t + T/2)$ describes, and vice versa for u_-. To form the ratio define the variables:

$$\begin{aligned} U(t) &= u_+(t) + u_-(t) \\ V(t) &= v_1(t) + v_2(t) \\ R(t) &= \frac{V(t) - U(t)}{V(t) + U(t)}. \end{aligned} \tag{A.3}$$

Plugging in and dividing the common terms $(N_0 e^{-t/\tau}/4)$,

$$R(t) = \frac{2(1 + A\cos(\omega_a t)) - e^{-T/2\tau}(1 + A\cos(\omega_a t + \omega_a T/2)) - e^{T/2\tau}(1 + A\cos(\omega_a t - \omega_a T/2))}{2(1 + A\cos(\omega_a t)) + e^{-T/2\tau}(1 + A\cos(\omega_a t + \omega_a T/2)) + e^{T/2\tau}(1 + A\cos(\omega_a t + \omega_a T/2))}. \tag{A.4}$$

Now set $\omega_a T/2 = \delta$, and note that T is really

$$\begin{aligned} T = T_{guess} &= \frac{2\pi}{\omega_a} + \Delta T, \\ \Delta T &= T_{guess} - T_{true}. \end{aligned} \tag{A.5}$$

Being explicit,

$$\delta = \frac{\omega_a}{2} T_{guess} = \frac{\omega_a}{2}(\frac{2\pi}{\omega_a} + \Delta T) = \pi + \pi \frac{\Delta T}{T_{true}} = \pi + \pi(\delta T), \tag{A.6}$$

and δ can be redefined as

$$\delta = \pi(\delta T), \tag{A.7}$$

by flipping the sign of any cosine terms that contain δ.

Then, using the trig identity

$$\cos(a \pm b) = \cos(a)\cos(b) \mp \sin(a)\sin(b) \tag{A.8}$$

so that

$$\begin{aligned} \cos(\omega_a t \pm \delta) &= \cos(\omega_a t)\cos\delta \mp \sin(\omega_a t)\sin\delta \\ &\approx \cos(\omega_a t)(1-\delta^2) \mp \sin(\omega_a t)\delta \\ &\approx \cos(\omega_a t), \end{aligned} \tag{A.9}$$

since $\delta \sim O(10^{-5})$, the ratio becomes

$$R(t) \approx \frac{2(1 + A\cos(\omega_a t)) - (1 - A\cos(\omega_a t))(e^{-T/2\tau} + e^{T/2\tau})}{2(1 + A\cos(\omega_a t)) + (1 - A\cos(\omega_a t))(e^{-T/2\tau} + e^{T/2\tau})}. \tag{A.10}$$

Expanding

$$e^{\pm T/2\tau} = 1 \pm \frac{T}{2\tau} + \frac{1}{2}\Big(\frac{T}{2\tau}\Big)^2 \pm \ldots, \tag{A.11}$$

repacing and simplifying,

$$R(t) \approx \frac{A\cos(\omega_a t) - C(1 - A\cos(\omega_a t))}{1 + C(1 - A\cos(\omega_a t))}, \tag{A.12}$$

where

$$C = \frac{1}{16}\Big(\frac{T}{\tau}\Big)^2 \approx 2.87 * 10^{-4}. \tag{A.13}$$

Using the expansion

$$f(x) = \frac{1}{1+x} = 1 - x + x^2 - \ldots, \quad |x| < 1, \tag{A.14}$$

and since C is small, the denominator can be manipulated such that

$$\begin{aligned} R(t) &\approx (A\cos(\omega_a t)) - C(1 - A\cos(\omega_a t)))(1 - C(1 - A\cos(\omega_a t))) \\ &\approx A\cos(\omega_a t) - C + CA^2\cos^2(\omega_a t), \end{aligned} \tag{A.15}$$

after dropping terms of $\mathcal{O}(C^2)$ and higher. In practice the last term is ommitted since it has a minimal effect on the fitted value of ω_a [**cite**], and one arrives at

$$R(t) \approx A\cos(\omega_a t) - C, \tag{A.16}$$

the conventional 3 parameter ratio function.

In order to avoid approximations one can instead weight the counts in the histograms as

$$u_+(t) : u_-(t) : v_1(t) : v_2(t) = e^{T/2\tau} : e^{-T/2\tau} : 1 : 1, \tag{A.17}$$

so that

$$\begin{aligned} u_+(t) &= \frac{e^{T/2\tau}}{2 + e^{T/2\tau} + e^{-T/2\tau}} N_5(t + T/2) \\ u_-(t) &= \frac{e^{-T/2\tau}}{2 + e^{T/2\tau} + e^{-T/2\tau}} N_5(t - T/2) \\ v_1(t) &= \frac{1}{2 + e^{T/2\tau} + e^{-T/2\tau}} N_5(t) \\ v_2(t) &= \frac{1}{2 + e^{T/2\tau} + e^{-T/2\tau}} N_5(t). \end{aligned} \tag{A.18}$$

(These factors out front aren't so far off from 1/4 since $e^{\pm T/2\tau} \approx e^{\pm 4.35/2*64.4} \approx 1.034, .967$.) Then instead $R(t)$ becomes

$$R(t) = \frac{2(1 + A\cos(\omega_a t)) - (1 - A\cos(\omega_a t + \delta)) - (1 - A\cos(\omega_a t - \delta))}{2(1 + A\cos(\omega_a t)) + (1 - A\cos(\omega_a t + \delta)) + (1 - A\cos(\omega_a t + \delta))}, \tag{A.19}$$

where the $e^{\pm T/2\tau}$ terms out front now cancel. Using Equation A.9 again and this time avoiding approximations in δ,

$$R(t) = \frac{2A\cos(\omega_a t)(1 + \cos\delta)}{4 + 2A\cos(\omega_a t)(1 - \cos\delta)}, \tag{A.20}$$

after simplifying. In the limit that

$$\delta = \pi(\delta T) \to 0 \tag{A.21}$$

since δT is small,

$$R(t) \approx A\cos(\omega_a t), \tag{A.22}$$

with the only approximation being made at $\mathcal{O}(\delta^2) \sim \mathcal{O}(10^{-10})$.

Finally, while the 3 parameter ratio function suffices for fits to data containing slow modulations, it does not suffice for faster oscillation features. In that case it is more useful to fit with the non-approximated or simplified version of the ratio,

$$\begin{aligned} R(t) &= \frac{v_1(t) + v_2(t) - u_+(t) - u_-(t)}{v_1(t) + v_2(t) + u_+(t) + u_-(t)}, \\ &= \frac{2f(t) - f_+(t) - f_-(t)}{2f(t) + f_+(t) + f_-(t)}, \end{aligned} \tag{A.23}$$

where

$$\begin{aligned} f(t) &= C(t)(1 + A\cos(\omega_a t + \phi)) \\ f_\pm(t) &= f(t \pm T_a/2), \end{aligned} \tag{A.24}$$

and $C(t)$ can encode any other effects in the data that need to be fitted for, such as the CBO,

$$C(t) = 1 + A_{cbo} e^{-t/\tau_{cbo}} \cos(\omega_{cbo} t + \phi_{cbo}). \tag{A.25}$$

Additionally, any other fit parameters such as A or ϕ can be made a fuction of t. Using the non-approximated form for the final fit function gives greater confidence in the fit results for the high precision ω_a extraction necessary for the experimental measurement.

Appendix B

Ratio Method Errors